


RESEARCH PAPER

 OPEN ACCESS  Check for updates

Feedback regulation of small RNA processing by the cleavage product

Svetlana Durica-Mitic and Boris Görke 

Department of Microbiology, Immunobiology and Genetics, Max F. Perutz Laboratories (MFPL), University of Vienna, Vienna Biocenter (VBC), Vienna, Austria

ABSTRACT

Many bacterial small RNAs (sRNAs) are processed resulting in variants with roles potentially distinct from the primary sRNAs. In *Enterobacteriaceae* sRNA GlmZ activates expression of *glmS* by base-pairing when the levels of glucosamine-6-phosphate (GlcN6P) are low. GlmS synthesizes GlcN6P, which is required for cell envelope biosynthesis. When dispensable, GlmZ is cleaved by RNase E in the base-pairing sequence. Processing requires protein RapZ, which binds GlmZ and recruits RNase E by interaction. Cleavage is counteracted by the homologous sRNA GlmY, which accumulates upon GlcN6P scarcity and sequesters RapZ. Here, we report a novel role for a processed sRNA. We observed that processing of GlmZ is never complete *in vivo*. Even upon RapZ overproduction, a fraction of GlmZ remains full-length, while the 5' cleavage product (GlmZ*) accumulates. GlmZ* retains all elements required for RapZ binding. Accordingly, GlmZ* can displace full-length GlmZ from RapZ and counteract processing *in vitro*. To mimic GlmZ* *in vivo*, sRNA chimeras were employed consisting of foreign 3' ends including a terminator fused to the 3' end of GlmZ*. *In vitro*, these chimeras perform indistinguishable from GlmZ*. Expression of the chimeras *in vivo* inhibited processing of endogenous GlmZ, causing moderate upregulation of GlmS synthesis. Hence, accumulation of GlmZ* prevents complete GlmZ turnover. This mechanism may serve to adjust a robust *glmS* basal expression level that is buffered against fluctuations in RapZ availability.

ARTICLE HISTORY

Received 5 March 2019
Revised 19 April 2019
Accepted 22 April 2019

KEYWORDS



Small RNA GlmZ; RNase E; adaptor protein RapZ; RNA processing; feedback regulation


Introduction

Bacterial *trans*-encoded small RNAs (sRNAs) cooperate extensively with ribonucleases (RNases) to exert their regulatory roles [1,2]. In Gram-negative bacteria, the endoribonuclease RNase E holds a key role, not only for bulk RNA turnover, but also for sRNA function [3,4]. Many sRNAs guide RNase E to destabilize their target RNAs [5–7], which often involves co-degradation of the base-paired sRNA [8–10]. Often, RNase E is also responsible for initiation of degradation of *trans*-encoded sRNAs when not base-paired [2]. However, RNase E also has important roles for sRNA biogenesis and maturation. Several sRNAs are known to be produced from the 3' region of protein coding genes, either through usage of an internal promoter or by RNase E catalyzed mRNA processing [11–13], and regulatory roles for sRNAs generated through the latter mechanism were demonstrated in various species including *E. coli* and *Salmonella* [14–17]. An additional class of sRNAs is autonomously transcribed, but undergoes maturation. RNase E converts these sRNAs into shorter stable variants that retain regulatory potential [18–21]. At least in one case, sRNA maturation was shown to be essential for regulation [12]. In addition, processing by RNase E may generate sRNA species with a target spectrum distinct from the genes regulated by the unprocessed sRNA [22]. sRNAs processed in the 5' region carry a 5' monophosphate converting them into preferred substrates for further degradation by RNase E. The sRNA 5' monophosphate may also promote

rapid target RNA degradation through interaction with the 5' sensing pocket in RNase E, thereby allosterically activating the enzyme [23]. Taken together, processed variants of sRNAs may have specific roles and properties deviating from the corresponding full-length sRNAs.

How RNase E selects its cleavage sites is weakly understood. A study mapping RNase E cleavage sites genome-wide proposed the degenerate cleavage motif RN|WUU [12], suggesting that additional elements such as RNA secondary structures contribute to RNase E recognition [24]. Indeed, in-depth analysis of sRNA MicL revealed that precise cleavage by RNase E is directed by two adjacent stem loop structures located 3' to the cleavage site [25]. Furthermore, dedicated adaptor proteins may be employed to mediate precise cleavage of sRNAs in a regulated manner. A prominent example is provided by the GlmY/GlmZ/RapZ circuit in *Enterobacteriaceae*, which controls synthesis of enzyme GlmS at the post-transcriptional level [26]. GlmS produces glucosamine-6-phosphate (GlcN6P), which is required for synthesis of cell envelope components peptidoglycan and LPS. When GlcN6P levels are low, the small RNA GlmZ base-pairs with the *glmS* 5'-UTR to activate translation, which concomitantly stabilizes the mRNA [27,28]. GlmZ is constitutively transcribed and regulated at the level of decay. When not required, the adaptor protein RapZ binds GlmZ and recruits RNase E through interaction to inactivate the sRNA by cleavage in the base-pairing region [29,30]. GlmZ consists of three stem loop structures, the central of which is decisive for RapZ binding and

CONTACT Boris Görke  boris.goerke@univie.ac.at  Department of Microbiology, Immunobiology and Genetics, Max F. Perutz Laboratories (MFPL), University of Vienna, Vienna Biocenter (VBC), Vienna, Austria

 Supplementary data for this article can be accessed [here](#)

© 2019 The Author(s). Published by Informa UK Limited, trading as Taylor & Francis Group. This is an Open Access article distributed under the terms of the Creative Commons Attribution License (<http://creativecommons.org/licenses/by/4.0/>), which permits unrestricted use, distribution, and reproduction in any medium, provided the original work is properly cited.

cleavage by RNase E that occurs 6 or 7 nt downstream of this structure [31]. Due to coinciding sites, binding of Hfq and cleavage by the RapZ/RNase E complex are mutually exclusive. Cleavage of GlmZ is regulated through employment of the homologous sRNA GlmY, which accumulates when the GlcN6P concentration decreases [32]. GlmY serves as decoy and sequesters RapZ thereby counteracting GlmZ processing, but is itself not cleaved by RNase E [30,31].

In the current study, we addressed whether the processed variant of GlmZ (subsequently designated GlmZ*) also has a role. We observed that processing of GlmZ is never complete *in vivo* suggesting that accumulation of GlmZ* limits ongoing GlmZ cleavage. Indeed, GlmZ* efficiently competes with full-length GlmZ for binding to RapZ. Accordingly, GlmZ* is capable of inhibiting cleavage of full-length GlmZ by RapZ/RNase E *in vitro*. Finally, expression of sRNA chimeras mimicking GlmZ* counteracted processing of endogenous GlmZ *in vivo* and caused a moderate upregulation of *glmS* expression, which was more pronounced in strains lacking decoy sRNA GlmY. We conclude, that the level of GlmZ* sets a threshold to prevent complete turnover of full-length GlmZ. This mechanism may serve to provide a robust basal level of *glmS* expression, which might be in particular important when the level of the decoy sRNA GlmY is low.

Results and discussion

Even extraordinary high RapZ levels do not trigger complete processing of GlmZ *in vivo*

In *wild type* cells grown to exponential phase, slightly more GlmZ* than full-length GlmZ is detectable in Northern analysis (Figure 1, lane 1 [30]). A *glmY* deletion has only a limited impact and shifts this ratio slightly in favour of GlmZ* as observed previously (Figure 1, lanes 3 and 4 [30,32]). Physiologically, GlmY accumulates and strongly counteracts GlmZ processing when cells experience GlcN6P scarcity [32,33]. Plasmid-driven overexpression of GlmY abolishes GlmZ processing and leads to strong upregulation of GlmS (Figure 1, lane 5), which is the consequence of sequestration of RapZ by GlmY [30]. A comparable result was obtained in the $\Delta rapZ$ mutant, reflecting that RapZ is absolutely required to guide GlmZ to processing by RNase E (Figure 1, lane 6 [30]). Complementation of the $\Delta rapZ$ mutant with a low copy plasmid carrying *rapZ* under control of the tightly regulated P_{BAD} promoter restores processing of GlmZ in the presence of the inducer arabinose (Figure 1, lanes 7–8). We performed a similar complementation experiment but used a plasmid with the IPTG-inducible P_{tac} promoter and a strong ribosomal binding site to overproduce RapZ to higher levels. This construct allows overproduction of RapZ, which carried an N-terminal Strep-tag in this case, to levels becoming visible even in total cell extracts analysed by SDS-PAGE/Coomassie staining. Strep-RapZ was already detectable in the absence of IPTG (due to leakiness of P_{tac} repression by LacI) and accumulated further in the presence of IPTG (Figure 1, bottom panel, lanes 9–10). Western blotting using antisera directed against RapZ or the Strep-tag validated this band as RapZ (Figure 1, panels 5 and 6, lanes 9–10). Interestingly, regardless of these high RapZ levels,

complete processing of GlmZ was not obtained (Figure 1, top panel, lanes 9–10). GlmZ* accumulated to high levels, whereas the level of full-length GlmZ remained basically unaffected (Figure 1, top panel, compare lanes 9–10 with lanes 1 and 8). Thus, the extent of GlmZ processing does not strictly correlate with the RapZ level and is limited by another factor. As it strongly accumulates upon RapZ overproduction, we reasoned that this factor might be GlmZ*.

GlmZ* counteracts cleavage of full-length GlmZ by inhibition of RapZ/GlmZ complex formation *in vitro*

So far, no condition has been identified that would enable complete processing of GlmZ *in vivo*. We previously showed that Hfq provides protection against cleavage by RapZ/RNase E by covering the RNase E cleavage site in GlmZ upon binding [31]. Accordingly, abundance of full-length GlmZ decreases in favour of GlmZ* in an *hfq* mutant. Nonetheless, a minor but significant fraction of GlmZ remains uncut even in the absence of Hfq [30]. The same is true for $\Delta glmY$ strains eliminating sequestration of RapZ by the decoy sRNA [32]. Taken together, GlmZ is not completely processed even when access of RapZ/RNase E to GlmZ is facilitated through elimination of Hfq or GlmY [30,32], or when RapZ is overproduced to high levels (Figure 1). The concomitant strong accumulation of GlmZ* in the latter case prompted us to inquire whether GlmZ* competes with full-length GlmZ for binding RapZ, thereby sequestering this protein and limiting cleavage of full-length GlmZ. Previous results have shown that RapZ requires the two 5'-terminal stem loop structures in GlmZ for binding, which are also retained in GlmZ* [31]. Accordingly, full-length and processed GlmZ are both bound by RapZ with comparable affinities [29,30]. Therefore, we tested whether GlmZ* is able to displace full-length GlmZ from complexes with RapZ and vice versa, which we addressed by EMSA. In this case, radioactively labelled full-length GlmZ as well as GlmZ* were pre-incubated with saturating amounts of RapZ to allow for binding and subsequently increasing concentrations of 'cold' GlmZ* and full-length GlmZ were added, respectively. Indeed, GlmZ* displaced full-length GlmZ from the RapZ complexes with similar efficiency as observed in the reverse assay, which addressed dissolution of RapZ/GlmZ* complexes by cold full-length GlmZ (Figure 2(a)). In conclusion, processed and full-length GlmZ compete with comparable efficiencies for getting access to RapZ.

Next, we tested whether GlmZ* is capable of counteracting cleavage of full-length GlmZ by RNase E/RapZ *in vitro*, as previously observed for GlmY [30]. To this end, radioactively labelled full-length GlmZ was incubated with purified RapZ and the catalytic domain of RNase E in the absence or presence of incremental concentrations of unlabelled GlmZ* or GlmY for comparison to follow GlmZ cleavage within 30 min reaction time. RapZ has no role for GlmZ processing in the absence of RNase E, whereas incubation of GlmZ with RNase E alone yielded unspecific cleavage products only (Figure 2(b), lanes 1–3). In agreement with previous data [30,31], accumulation of properly processed GlmZ could only be observed in the presence of both, RapZ and RNase E-NTD (Figure 2(b), lane 4). Indeed, additional presence of GlmZ* in the assay inhibited GlmZ cleavage when supplied at

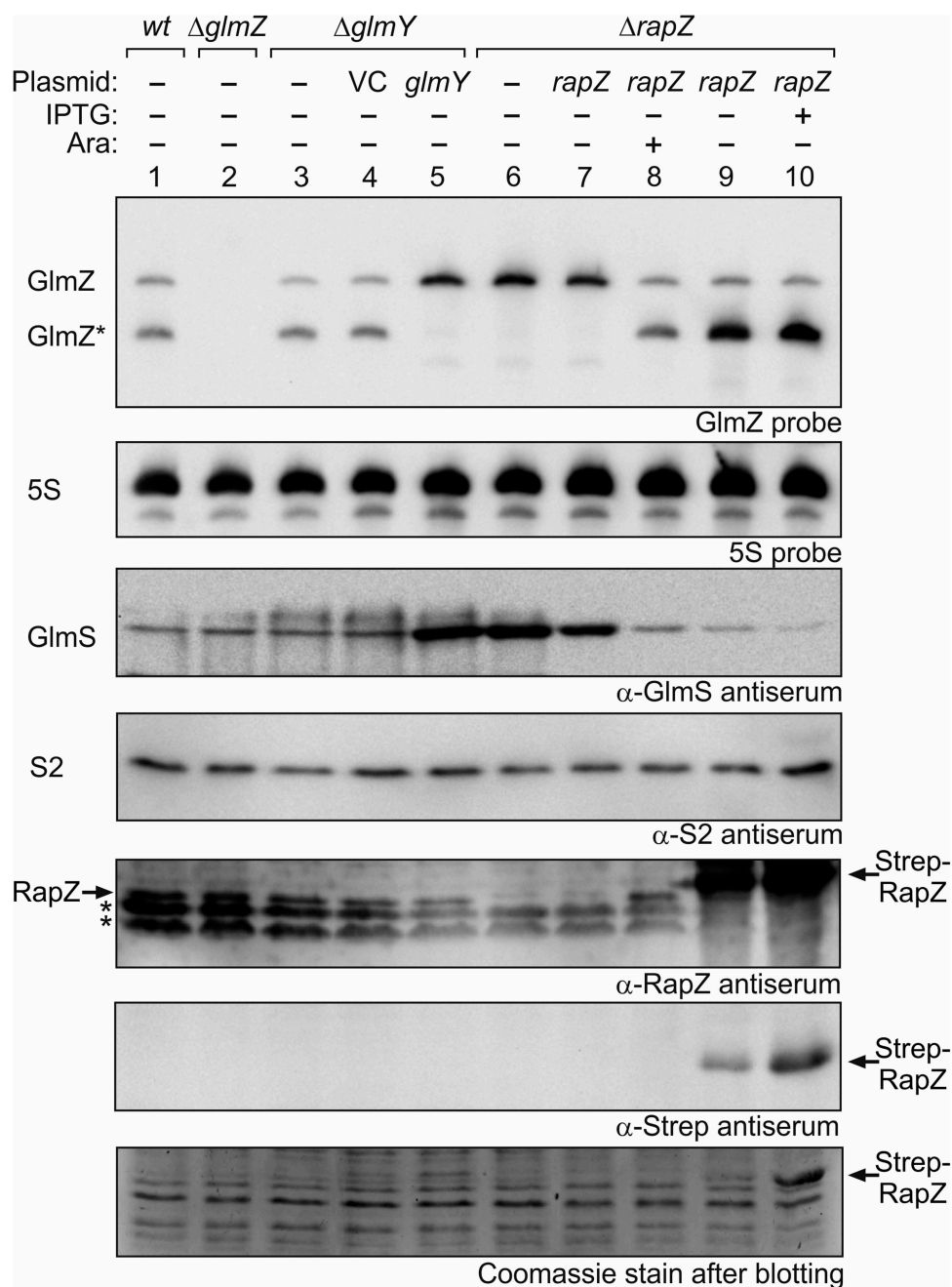


Figure 1. High RapZ concentrations trigger accumulation of processed GlmZ but do not completely turn over full-length GlmZ. Northern analyses addressing abundance of full-length and processed GlmZ in various genetic backgrounds (top panel) and the consequences for GlmS protein levels as detected by immunoblot analyses (panel 3 from top). Strains R1279 (*wild type*, lane 1), Z45 ($\Delta glmZ$, lane 2), Z95 ($\Delta glmY$, lanes 3–5) and Z37 ($\Delta rapZ$, lanes 6–10) were used, which occasionally harboured the following plasmids: pBR-plac (VC = vector control; lane 4), pYG83 (lane 5), pBGG61 (lanes 7, 8), pBGG164 (lanes 9, 10). The bacteria were grown to exponential phase and harvested for isolation of total RNA and total protein, respectively. 5 μ g of the total RNA preparations were subjected to Northern analysis using probes directed against GlmZ (top panel) and 5S rRNA as loading control (second panel from top). Total protein extracts were separated by SDS PAGE and analysed by Western blotting using antisera directed against GlmS (panel 3 from top), ribosomal protein S2 as loading control (panel 4 from top), RapZ (panel 5 from top), and the Strep epitope (panel 6 from top). Non-specific signals are indicated with asterisks. Following blotting, the SDS PAA gel was stained with Coomassie blue to visualize overproduced Strep-RapZ and to provide a further loading control (bottom panel). Arabinose and IPTG were added to the cultures for induction of *rapZ* expression as indicated.

concentrations of ≥ 16 nM (Figure 2(b), lanes 7–9). Inhibition of GlmZ cleavage by GlmZ* was less efficient as compared to GlmY, which impeded GlmZ processing already at a concentration of ≥ 8 nM (Figure 2(b), lanes 10–14). Taken together, GlmZ* competes with full-length GlmZ for RapZ binding,

thereby counteracting GlmZ processing *in vitro*, but with a somewhat lower efficiency than observed for GlmY.

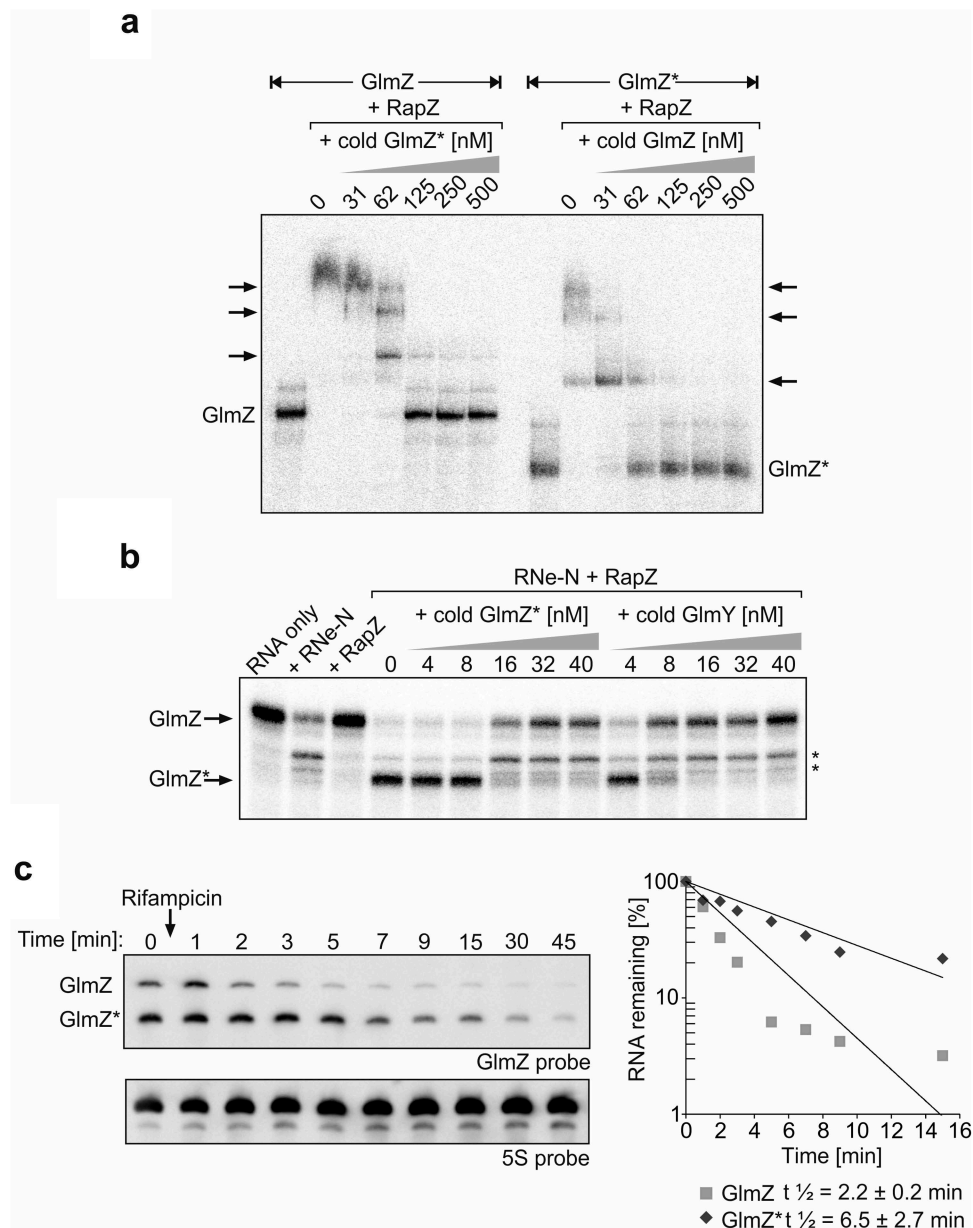


Figure 2. GlmZ* competes efficiently with full-length GlmZ for binding RapZ and inhibits cleavage of full-length GlmZ by RNase E *in vitro*. (a) EMSA demonstrating that full-length and processed GlmZ can displace each other from complexes with RapZ. α - 32 P-UTP labelled full-length GlmZ (left) and GlmZ* (right) were pre-incubated with 1500 nM RapZ to achieve complex formation. Subsequently, incremental concentrations of non-labelled GlmZ* (left) and full-length GlmZ (right) were added, respectively. Following an additional incubation step, binding reactions were separated by non-denaturing gel electrophoresis and gels were analysed by phospho-imaging. (b) *In vitro* cleavage assay demonstrating that GlmZ* inhibits cleavage of full-length GlmZ by RapZ/RNase E. α - 32 P-UTP labelled full-length GlmZ was incubated alone ('RNA only', lane 1) or solely with 25 nM RNase E-NTD (lane 2) or 20 nM RapZ (lane 3), or with both proteins simultaneously (lanes 4–14). In the latter case, various concentrations of non-labelled GlmZ* or GlmY were added as indicated. Following incubation, the reaction products were separated on denaturing PAA gels, which were subsequently analysed by phospho-imaging. Non-specific cleavage products are indicated by asterisks on the right. (c) Left: Northern blot addressing half-life of full-length and processed GlmZ following treatment with rifampicin. *Wild type* strain R1279 was grown to exponential phase and treated with rifampicin to stop transcription. At indicated times samples were removed for isolation of total RNA, which was analysed by Northern blotting using probes directed against GlmZ (top) and the 5S rRNA (bottom). Right: Semi-logarithmic plots of GlmZ* and full-length GlmZ decay for half-life determination. RNA signal intensities were normalized to 5S signals and plotted semi-logarithmically in percent against time. The graph shows the average values of three independent experiments.

Design of sRNA chimeras mimicking GlmZ*

We wanted to complement the *in vitro* observations with evidence that accumulation of GlmZ* indeed limits ongoing processing of full-length GlmZ *in vivo*. As termination is required, it is impossible to generate primary transcripts *in vivo* corresponding to GlmZ*. Another possibility to increase abundance of GlmZ* is to block its degradation. GlmZ half-life

measurements following rifampicin treatment indicated that GlmZ* is more stable as compared to full-length GlmZ (Figure 2(c) left). Quantification revealed $t_{1/2}$ values of 2.2 ± 0.2 min for full-length GlmZ and 6.5 ± 2.7 min for GlmZ* in the *wild type* strain (Figure 2(c) right). The long half-life explains why GlmZ* remains detectable under steady state conditions and accumulates when processing is stimulated

through elevated RapZ levels (see Figure 1). Consequently, GlmZ* exists long enough allowing it to compete with full-length GlmZ for interaction with RapZ. Unfortunately, our search for RNases responsible for turning over GlmZ* was unsuccessful. Absence of the major RNases PNPase, RNase III, RNase G, RNase R or RNase II did not cause accumulation of GlmZ*, respectively (Figure S1). Thus, these RNases have apparently no role for turnover of GlmZ* or redundant enzymes compensate. Therefore, we sought to mimic GlmZ* by using chimeras consisting of a heterologous transcriptional terminator fused to the 3' end of GlmZ*. Such chimeras should fulfil two criteria: First, they must possess sizes allowing for their discrimination from endogenously produced full-length

GlmZ and GlmZ* in Northern analyses. Second, they should not themselves be cleaved by RapZ/RNase E as this would liberate the GlmZ portion that is indistinguishable from GlmZ* derived from endogenously encoded GlmZ. We have previously shown that RNase E cleaves GlmZ at a fixed position in the single stranded region (i.e. 6 or 7 nucleotides) downstream of the second stem loop regardless of sequence composition at the cleavage site (Figure 3(a) left [31]). As sequence variation has no impact, we reasoned to prevent cleavage by reducing or removing the single-stranded region following the second stem loop. Lastly, we constructed three different chimeras, all consisting of the two first stem loops of GlmZ at the 5' end and the transcriptional terminator of the *trpA* gene at

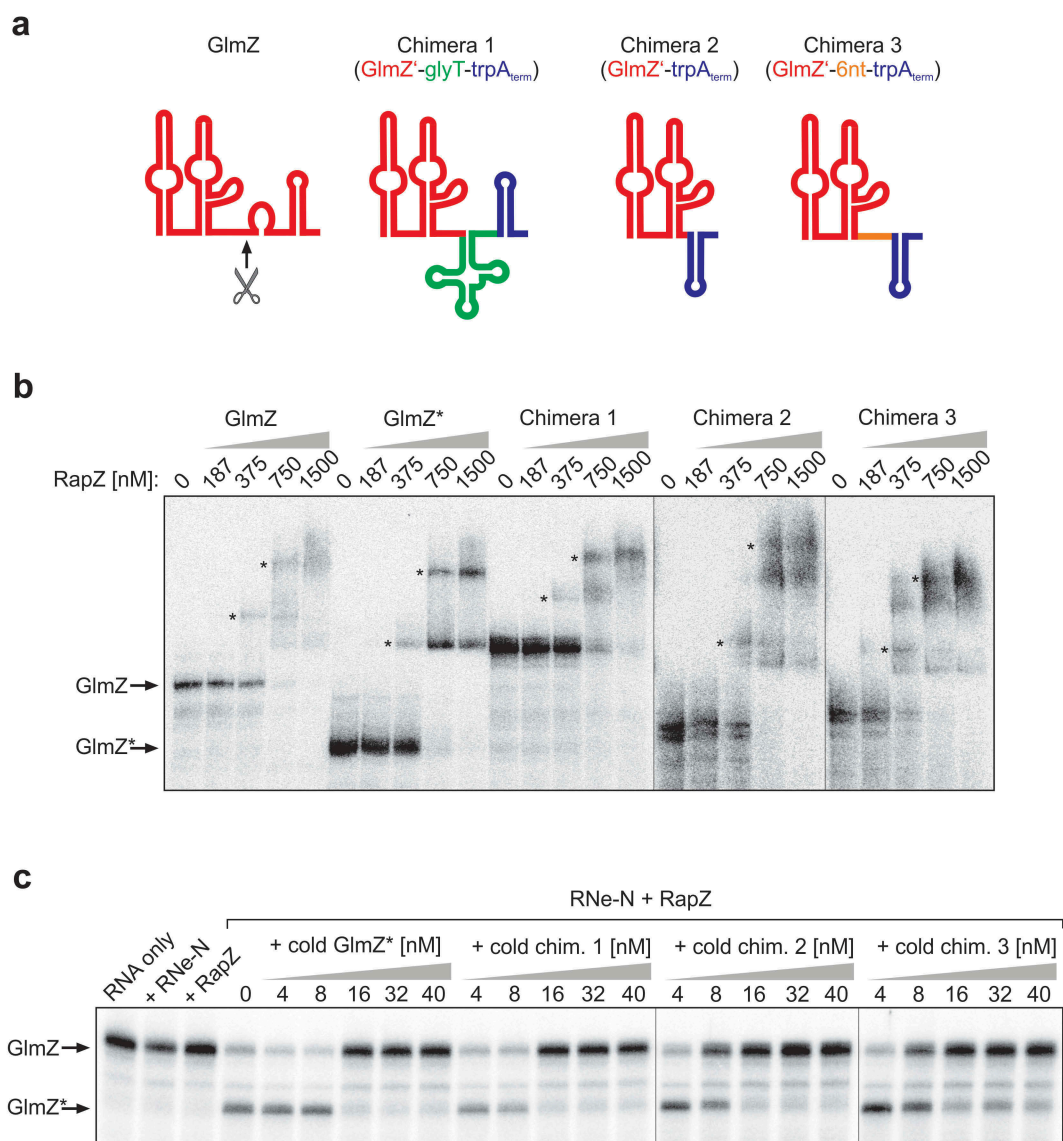


Figure 3. sRNA chimeras mimicking GlmZ* bind RapZ efficiently and counteract cleavage of full-length GlmZ by RNase E *in vitro*. (a) Schematic representation of the sRNA chimeras used to mimic GlmZ*. Parts derived from GlmZ are depicted in red, the *trpA* terminator is shown in blue, the *glyT* tRNA in green and the 6 nt BgIII site insertion in chimera 3 is in orange. The structure of full-length GlmZ including location of the processing site (marked with an arrow) is shown for comparison. (b) EMSA demonstrating that RapZ binds GlmZ, GlmZ* and the sRNA chimeras with comparable affinities. α -³²P-UTP labelled full-length GlmZ, GlmZ* and sRNA chimeras were incubated with incremental concentrations of RapZ, respectively, and binding reactions were subsequently separated on non-denaturing PAA gels and analysed by phospho-imaging. In case of chimeras 2 and 3, premature transcription termination additionally generated slightly shorter sRNA variants, which were similarly efficient bound as the full-length sRNAs and contributed to additional sRNA/RapZ complexes. It should be noted that complete binding of GlmZ required higher RapZ concentrations as previously reported [30,31], which may be attributed to the individual RapZ protein preparation used. (c) *In vitro* cleavage assay demonstrating that the various sRNA chimeras impede processing of full-length GlmZ by RapZ/RNase E similarly efficient as GlmZ*. Same assay as in Figure 2B, but as a difference the various non-labelled sRNA chimeras were added.

the 3' end, but with different sequences between these modules to also account for a possible steric hindrance of RapZ binding by the adjacent terminator (Figure 3(a)). Chimera 1 carries the highly structured *glyT* tRNA inserted between the sequences corresponding to GlmZ* (nt 1–155) and the *trpA* terminator, respectively (Figure 3(a)). In chimera 2, the *trpA* terminator was fused directly to the 3' end of the central stem loop of GlmZ. Chimera 3 is similar, but additionally carries 6 foreign nucleotides between the central stem loop of GlmZ and the *trpA* terminator (Figure 3(a)).

GlmZ chimeras mimicking GlmZ* inhibit processing of full-length GlmZ in vitro and in vivo through sequestration of RapZ

First, we tested whether the various sRNA chimeras are efficiently bound by RapZ and able to counteract processing of GlmZ by RapZ/RNase E *in vitro*. EMSA revealed no major differences in the binding properties between full-length GlmZ, GlmZ* and the chimeras: All these RNAs are bound by RapZ with comparable affinities (Figure 3(b)). Depending on the RapZ concentration multiple higher weight complexes became detectable that may refer to RapZ oligomers binding different numbers of GlmZ molecules. We recently showed that active RapZ is a tetramer possessing four RNA-binding surfaces [29]. When tested in the cleavage assay *in vitro*, the various chimeras inhibited processing of GlmZ by RapZ/RNase E similarly efficient as GlmZ*. In all cases, at least 16 nM of the respective competitor sRNA were required to completely block cleavage of GlmZ in an assay containing 25 nM RNase E-NTD and 20 nM RapZ (Figure 3(c)).

To test whether the various chimeras counteract processing of GlmZ *in vivo*, the fusion RNAs were expressed from plasmid pBR-plac under control of the $P_{LlacO-1}$ promoter. *Wild type* and $\Delta glmZ$ strains harbouring these plasmids were grown to the exponential growth phase and total RNAs were isolated and subjected to Northern analysis using a probe capable of detecting both endogenous GlmZ as well as the various chimeras. Assessing the RNAs in the $\Delta glmZ$ strain showed that all chimeras migrated in the gel at positions different from full-length and processed GlmZ allowing for their discrimination (Figure 4(a), compare lanes 8–10 with lane 1). Moreover, no processing products in the size of GlmZ* became detectable, confirming that RNase E is unable to cleave the chimeras downstream of the central stem loop. Importantly, in the *wild type* strain, expression of the various chimeras caused disappearance of the processed form of endogenous GlmZ and simultaneously led to a slight increase in abundance of full-length GlmZ (Figure 4(a), compare lanes 3–5 with lane 1). Analysis of these samples using a probe specific for the 3' end of GlmZ corroborated increased abundance of full-length GlmZ upon expression of the sRNA chimeras (Figure S2, compare lanes 3–5 with lane 1).

To determine whether the latter increase in abundance results from slower GlmZ degradation, GlmZ half-life in the strain expressing chimera 3 was determined (Figure 4(b)). Notably, presence of chimera 3 led to a pronounced increase of full-length GlmZ half-life as compared to the strain carrying the empty plasmid (Figure 4(b), compare panels 1 and 3

from top). To corroborate once again that the slower migrating band corresponds to full-length GlmZ, the total RNA (isolated at $t = 0$) was separated alongside total RNAs isolated from the *wild type* strain containing no plasmid or the empty vector (Figure 4(b) bottom). Comparison of signal intensities confirmed up-regulation of full-length GlmZ in the strain producing chimera 3 once again. Taken together, our results indicate that the sRNA chimeras mimicking GlmZ* counteract RapZ-mediated cleavage of full-length GlmZ *in vitro* and *in vivo*, thereby increasing GlmZ steady state levels.

Expression of the sRNA chimeras mimicking GlmZ* augments GlmS synthesis

To investigate the impact of the sRNA chimeras on *glmS* expression, we first assessed GlmS protein levels in the *wild type* strain. Western blotting analysis of total protein extracts revealed somewhat increased GlmS levels in cells expressing the sRNA chimeras as compared to the empty plasmid control (Figure 4(d), compare lane 1 with lanes 3–5). Quantification of signal intensities and their normalization to S2 protein levels indicates a two- to four-fold increase relative to the control (Figure S3). However, upregulation of GlmS levels by the sRNA chimeras was less pronounced as compared to cells overproducing GlmZ, which can directly activate *glmS* translation through base-pairing (Figure 4(d), compare lanes 2 with 3–5; Figure S3). To confirm the effects of the sRNA chimeras on *glmS* expression, we used strains carrying an ectopic *glmS'-lacZ* reporter fusion in the chromosome. In addition, these strains also harboured the plasmids encoding the various GlmZ chimeras or GlmZ or GlmY for comparison, respectively. Samples were harvested for determination of β -galactosidase activities as well as for extraction of RNA. Northern blotting of total RNAs proved once again that the sRNA chimeras counteract processing of endogenous GlmZ (Figure S4). Plasmid-driven expression of GlmY upregulated *glmS'-lacZ* expression 12-fold as compared to the strain carrying the empty plasmid, whereas overexpression of GlmZ increased enzyme activities 5.2-fold (Figure 4(c) top, columns 1–3), which is in agreement with previous results [31]. Expression of the various sRNA chimeras led to a minor, that is ~ 1.5 -fold upregulation of *glmS* expression (Figure 4(c) top, compare columns 4–6 with 1).

However, it is reasonable to assume that the endogenous sRNA GlmY, whose levels are determined by the intracellular GlcN6P concentration [32,33], may compensate in the latter case for most of the effects generated by the sRNA chimeras. That is, upregulation of GlmS by the sRNA chimeras may increase the GlcN6P concentration, which will in turn decrease the level of decoy sRNA GlmY, thereby redirecting RapZ to recruit more GlmZ molecules to processing. To learn whether the latter feedback mechanism that essentially provides GlcN6P homeostasis indeed masks the regulatory effects caused by the sRNA chimeras, we expressed the sRNA chimeras in a $\Delta glmY$ mutant. Indeed, in this case, presence of the various sRNA chimeras had a stronger impact, increasing *glmS'-lacZ* expression two- to three-fold and leading to four- to five-fold higher GlmS protein levels (Figure 4(c) bottom diagram; Figure 4(d), lanes 6–10; Figure S3).

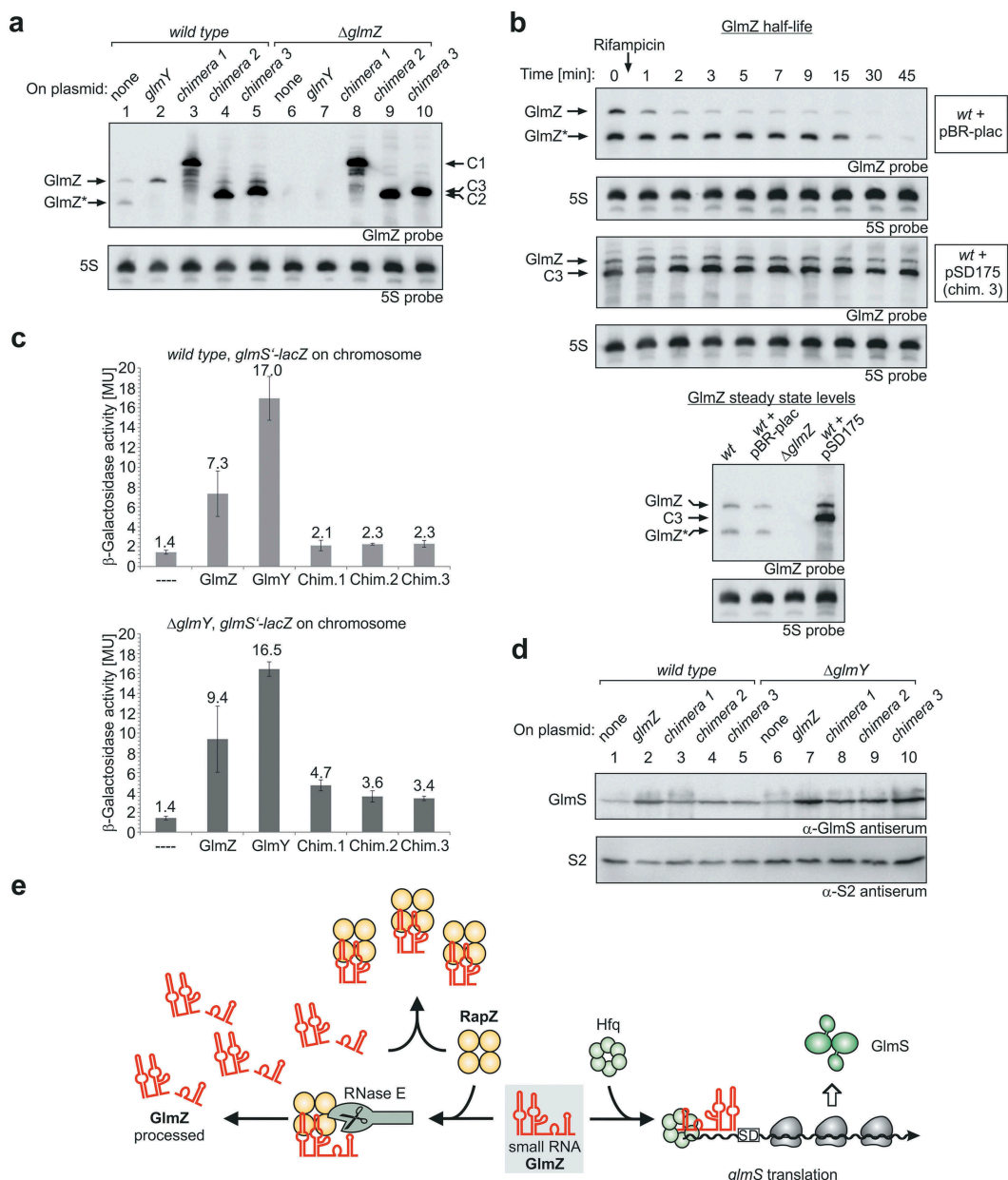


Figure 4. The sRNA chimeras mimicking GlmZ* counteract GlmZ processing *in vivo* thereby augmenting GlmS levels. (a) Plasmid-driven expression of the sRNA chimeras inhibits processing of endogenously encoded GlmZ. Strains R1279 (*wild type*, lanes 1–5) and strain Z45 ($\Delta glmZ$, lanes 6–10) harbouring plasmids encoding GlmY (pYG83, lanes 2 and 7), sRNA chimera 1 (pSD164, lanes 3 and 8), chimera 2 (pSD174, lanes 4 and 9), chimera 3 (pSD175, lanes 5 and 10) or the empty plasmid pBR-plac (lanes 1 and 6) were grown in LB to exponential phase for isolation of total RNA. 4 μ g total RNA each were analysed by Northern blotting using probes directed against GlmZ (top panel) and 5S rRNA (bottom panel). (b) sRNA chimera 3 counteracts degradation of full-length GlmZ. Northern blot addressing decay of full-length GlmZ in *wild type* strain R1279 in the presence of the empty plasmid pBR-plac (top panel) or plasmid pSD175 encoding chimera 3 (third panel from top). The transformants were grown to exponential phase and treated with rifampicin to stop transcription. Samples were removed at indicated times for isolation of total RNA, which was analysed by Northern blotting using probes directed against GlmZ and the 5S rRNA. To verify that the slower migrating band detected for transformant R1279/pSD175 corresponds to full-length GlmZ, the total RNA sample obtained before rifampicin addition (time 0) was analysed by Northern blotting (bottom panel) alongside total RNA samples of *wild type* strain R1279 (lane 1), R1279 carrying the empty plasmid pBR-plac (lane 2) and of the $\Delta glmZ$ mutant strain Z45 (lane 3). (c) Expression of the sRNA chimeras increases expression of a *glmS*-*lacZ* reporter fusion, which becomes more pronounced in a $\Delta glmY$ mutant strain. Strains Z8 (*wild type*) and Z884 ($\Delta glmY$) were employed, which carry a *glmS*-*lacZ* fusion integrated into the $\lambda attB$ site on the chromosome. The strains harboured the plasmids described in (a) as indicated. Additionally, transformants carrying plasmid pYG84 overexpressing GlmZ were included for comparison. (d) Effect of the sRNA chimeras on GlmS protein levels. Protein extracts were prepared from the *wild type* strain R1279 and the $\Delta glmY$ mutant strain Z95, which harboured plasmid pBR-plac (empty plasmid, lanes 1 and 6), pYG84 (GlmZ, lanes 2 and 7), pSD164 (chimera 1, lanes 3 and 8), pSD174 (chimera 2, lanes 4 and 9) or pSD175 (chimera 3, lanes 5 and 10). The extracts were subjected to Western blotting using antisera against GlmS (top panel) and S2 protein (bottom panel). (e) Model illustrating feedback regulation of GlmZ processing by processed GlmZ. Tetrameric RapZ (yellow) recruits RNase E (grey) to elicit cleavage of bound full-length GlmZ. Processed GlmZ retains the elements required for interaction with RapZ and sequesters RapZ when accumulating to high levels. This reduces ongoing processing of GlmZ, which is then free to associate with Hfq (green hexamer) and to stimulate *glmS* expression by base-pairing. This mechanism may absorb fluctuations in RapZ and RNase E availabilities thereby setting a robust basal *glmS* expression level.

Taken together, our data show that accumulation of an RNA corresponding to the processed form of GlmZ limits further processing of full-length GlmZ via sequestration of RapZ (Figure 4(e)). Thus, a sRNA cleavage product feedback regulates its own production via processing, which is a novel activity for a processed sRNA in bacteria. This feedback regulation may serve to buffer noise in RapZ and RNase E availabilities, thereby ensuring that a low basal level of the essential enzyme GlmS is always maintained (Figure 4(e)). This mechanism may be in particular important when GlmY levels are low, e.g. when the QseE/QseG/QseF three-component system, which controls *glmY* transcription, is in the OFF state [34,35]. Under these conditions, accumulation of GlmZ* may limit further processing of full-length GlmZ thereby maintaining a robust GlmS basal level. Interestingly, a similar regulatory scenario has also been proposed for human microRNAs [36]. In this case, miRNAs such as miR-21-5p were shown to inhibit their own biogenesis from the corresponding miRNA precursors, at least *in vitro*. Mechanistically, it is speculated that this regulation involves binding of the mature miRNA to Dicer, similar to the mechanism described here, which relies on binding of GlmZ* to RapZ. Thus, autoregulatory loops in which processed RNAs control their own production by binding to the processing enzymes could represent a widespread principle operating in all domains of life.

Materials and methods

Strains, plasmids and growth conditions

E. coli strains were routinely grown in Lysogeny broth (LB medium) at 37°C under agitation (165 rpm). When required, antibiotics were added at following concentrations: ampicillin (100 µg/ml), kanamycin (30 µg/ml), spectinomycin (50 µg/ml) and chloramphenicol (15 µg/ml). Expression of genes controlled by P_{Ara} promoter was induced by 0.2% arabinose and of genes controlled by P_{tac} or $P_{LlacO-1}$ promoter with 1 mM IPTG. *E. coli* strains and plasmids used in this study are described in Table 1 and oligonucleotides are listed in Table S1 under 'Supplemental Material'. Strain Z946 was constructed by transducing the *pnp::Tn5* allele of strain JC357 into strain Z854 using phage T4GT7 [37]. Construction of recombinant plasmids is described under 'Supplemental Material'.

RNA extraction, Northern blotting and sRNA half-life determination

Total RNA was extracted from exponentially growing cells using the ReliaPrep RNA Cell Miniprep System (Promega). For determination of GlmZ half-life, 500 µg/ml rifampicin was added to the culture. A sample harvested at the time of rifampicin addition corresponded to $t = 0$ min. Additional samples following rifampicin addition were collected for RNA extraction at the times indicated in Figure 2(c). Isolated total RNA was mixed with 2× RNA loading dye (95% formamide, 0.5 mM EDTA, 0.025% SDS, 0.025% bromophenol blue, 0.025% xylene cyanol) and separated by gel electrophoresis under denaturing conditions (7M urea, 6% acrylamide,

1× TBE) in 0.5× TBE as running buffer. Afterwards, RNA was transferred to a positively charged nylon membrane (Hybond H⁺; GE Healthcare) via electroblotting in 0.5× TBE for 1 h at 120 mA and crosslinked by exposure to 254 nm UV radiation. Digoxigenin (DIG)-labelled RNA probes were generated by *in vitro* transcription using T7 RNA polymerase (NEB) and DIG RNA labelling mix (Roche Diagnostics). Templates for probe synthesis were generated by PCR using primers BG230/BG231 for *glmZ*, BG1795/BG1796 for the *glmZ* 3'-end (nt 153–202) and BG287/BG288 for *rrfD*. Signal detection was achieved using an anti-DIG AP-conjugated antibody and CDP* as substrate, following the manufacturer's instructions (Roche Diagnostics). Signals were quantified using software ImageQuant TL 8.1 (GE Healthcare).

SDS-PAGE and Western blotting

Total protein extracts were prepared in SDS sample buffer and samples corresponding to 0.0625 OD₆₀₀ units of the cultures were separated on 12.5% SDS-polyacrylamide gels, respectively. Subsequently, proteins were transferred to a PVDF membrane (Amersham) via semidry blotting (PeqLab, 90 min at 120 mA). Following blotting, the SDS-PAA gels were stained with Coomassie Brilliant Blue R-250. The PVDF membranes were incubated with the required primary antisera (S2 antiserum diluted 1:5000; GlmS antiserum diluted 1:10,000 [38]; RapZ antiserum diluted 1:3000 [30]; anti-Strep antiserum diluted 1:20,000 (Promokine)) at 4°C overnight. The primary antibodies were detected by using rabbit IgG-AP conjugated secondary antibodies (Promega) diluted 1:100,000 and CDP* as substrate (Roche Diagnostics).

Protein purification

Strep-RapZ and the His-tagged catalytic domain of RNase E (aa 1–529) were overproduced in strain Z106 lacking endogenous *glmY* and *glmZ* genes using plasmids pBGG164 and pSD23, respectively. The proteins were subsequently purified as described previously with minor modifications for Strep-RapZ [30,31]. Modifications include cell lysis by sonication, clearing of the lysate by centrifugation at 14,000 rpm (1 h, 4°C) and omission of dialysis. Purified proteins were mixed with glycerol (5% v/v final concentration), shock-frozen and stored at –80°C until use.

In vitro transcription and labelling of small RNAs

Generation of ³²P-UTP labelled sRNAs *in vitro* is described under 'Supplemental Material'.

EMSA

EMSAs were carried out as previously described [31]. Binding reactions were performed in 1× binding buffer (10 mM Tris-HCl pH 7.0, 100 mM KCl, 10 mM MgCl₂) in a volume of 10 µl. The radiolabelled sRNA was mixed with 1 µg of yeast tRNA (Ambion), heat-denatured and briefly chilled on ice. Subsequently, appropriate RapZ protein dilutions (prepared in binding buffer) were added and samples were incubated for 30 min at 30°C. Thereafter, 2 µl of 5× native loading buffer (50% glycerol, 0.5

Table 1. Strains and plasmids used in this study.

Name	Genotype or relevant structure ^a	Reference
Strains:		
BW25113	$\Delta(\text{araD-araB})567$, $\Delta(\text{lacZ4787}::\text{rrnB-3})$, λ^- , rph-1 , $\Delta(\text{rhaD-rhaB})568$, hsdR514	[39]
IBPC633	as N3433, but rnc105 , $\text{nadB51}::\text{Tn10}$ (<i>tet</i>)	[40]
IBPC935	as N3433, but $\text{rng}::\text{cat}$	[41]
JC357	$F^- \text{argG6}$, metB1 , his1 , leu6 , mtl2 , xyl7 , malA1 , gal6 , lacY1 , tonA2 , tsx1 , λ^R , λ^- , supE44 , rpsL , recA , $\text{pnp}::\text{Tn5}$ (kan^R)	[42]
JW1279	as BW25113, but $\Delta\text{rnb-723}::\text{kan}$	[39]
JW5741	as BW25113, but $\Delta\text{rrn-729}::\text{kan}$	[39]
N3433	HfrH, lacZ43 , λ^- , relA1 , spoT1 , thi1	[43]
R1279	CSH50 $\Delta(\text{pho-bgl})201$, $\Delta(\text{lac-pro})$, ara , thi	[44]
XL1-blue	recA1 , endA1 , gyrA96 , thi-1 , hsdR17 , relA1 , supE44 , lac , $F[\text{proAB lac}^q \text{ lacZ}\Delta\text{M15 Tn10}]$	Laboratory stock
Z8	as R1279, but $\text{attB}::[\text{aadA}$, $\text{glmS-5}::\text{lacZ}]$, strp^R , $F'(\text{lac}^q)$	[28]
Z37	as R1279, but ΔrapZ	[28]
Z39	as R1279, but ΔglmZ , $\text{attB}::[\text{aadA}$, $\text{glmS-5}::\text{lacZ}]$, strp^R , $F'(\text{lac}^q)$	[31]
Z45	as R1279, but ΔglmZ	[28]
Z95	as R1279, but $\Delta\text{glmY}::\text{cat}$	[32]
Z106	as R1279, but ΔglmZ , ΔglmY	[30]
Z854	MG1655 rph^+ , ilvG^+ , ΔlacZ , $\lambda\text{attB}::[\text{aadA}$ (spec^R), $\text{glmS-5}::\text{lacZ}]$	[33]
Z884	as R1279, but ΔglmY , $\text{attB}::[\text{aadA}$, $\text{glmS-5}::\text{lacZ}]$, strp^R , $F'(\text{lac}^q)$	[31]
Z946	as Z854, but $\text{pnp}::\text{Tn5}$ (kan^R)	T4GT7 (JC357) → Z854; this work
Plasmids:		
pACA-RNA43 ^{SD}	3'-terminal 54 nts of <i>rrnB</i> followed by <i>glyT</i> and the <i>trpA</i> terminator in pBAD33	[45]
pBAD33	P_{AraC} , MCS 2, <i>cat</i> , <i>ori</i> p15A	[46]
pBGG61	<i>rapZ</i> (-17 to +855) under P_{AraC} control in pBAD33	[30]
pBGG164	<i>strep-rapZ</i> under P_{tac} control, lac^q , <i>bla</i> , <i>ori</i> ColEI	[47]
pBGG190	$\text{His}_{10}\text{-ptsN}$ under P_{tac} control, lac^q , <i>bla</i> , <i>ori</i> ColEI	[48]
pBGG237	<i>Strep-tag</i> under P_{tac} control, lac^q , <i>bla</i> , <i>ori</i> ColEI	[47]
pBR-plac	IPTG inducible artificial $P_{LlacO-1}$ promoter in pBR322; allows to start sRNA transcription at authentic +1 position	[49]
pRne529-N	$\text{His}_5\text{-rne}$ (+1 to +1587) in pET16b, <i>bla</i> , <i>ori</i> ColEI	[50]
pSD23	$\text{His}_{10}\text{-rne}$ (+1 to +1587) under P_{tac} control, lac^q , <i>bla</i> , <i>ori</i> ColEI	this work
pSD164	<i>glmZ</i> (1-155)- <i>glyT-trpA</i> _{term} fusion in pBR-plac	this work
pSD174	<i>glmZ</i> (1-146)- <i>trpA</i> _{term} fusion in pBR-plac	this work
pSD175	<i>glmZ</i> (1-146)-BgIII- <i>trpA</i> _{term} fusion in pBR-plac	this work
pYG83	<i>glmY</i> in pBR-plac	[31]
pYG84	<i>glmZ</i> in pBR-plac	[31]
pYG135	<i>strep-rne</i> (+1 to +1587) under P_{tac} control, lac^q , <i>bla</i> , <i>ori</i> ColEI	this work

^aORI: origin of replication; MCS: multiple cloning site

TBE, 0.2% bromophenol blue) were added and samples were separated on native polyacrylamide gels (6% PAA, 1× TBE) for 3 h at 4°C and 300 V using 0.5× TBE as running buffer. In case of competitive binding assays (Figure 2(a)), the radiolabelled sRNA and appropriate RapZ amounts were first co-incubated for 15 min at 30°C to allow for complex formation. Afterwards, non-radiolabelled competitor RNA was added in various concentrations and incubation was continued for 15 min at 30°C. Signals were detected by phospho-imaging (Typhoon FLA 9000, GE Healthcare).

RNase E cleavage assay

RNase E *in vitro* cleavage assays were performed in 1× reaction buffer (25 mM Tris/HCl pH 7.5, 50 mM NaCl, 50 mM KCl, 10 mM MgCl₂, 1 mM DTT) in a final volume of 10 μl as described earlier [31]. Briefly, radiolabelled GlmZ was mixed with 1 μg yeast tRNA (Ambion) and cold competitor RNA where appropriate. The RNA mix was heat-denatured, chilled on ice and incubated at 30°C for 5 min to allow for RNA folding. Afterwards, 20 nM RapZ was added and the samples were further incubated for 10 min at 30°C. Subsequently, 25 nM RNase E was added and incubation was continued for 30 min. The reactions were stopped by addition of 0.2 U proteinase K (NEB) and proteinase K buffer (100 mM Tris/HCl pH 7.5, 12.5 mM EDTA, 150 mM NaCl, 1% SDS) and incubation at 50°C for 30 min. Following the addition of 1 volume 2× RNA loading dye (95% formamide, 0.5 mM EDTA, 0.025% SDS, 0.025% bromophenol blue, 0.025% xylene cyanol) samples were separated on denaturing

polyacrylamide gels (6% PAA, 7M urea, 1× TBE). Dried gels were analysed by phospho-imaging.

Determination of β-galactosidase activity

β-Galactosidase activity assays were performed as previously described [51]. Shown values are the average of at least three measurements from independent cultures.

Acknowledgments

We thank Isabella Moll for providing S2 antiserum and plasmid pACA-RNA43^{SD}, Bernard Badet for the GlmS antiserum and Yvonne Göpel for construction of plasmid pYG135. We are grateful to Eliane Hajnsdorf for the gift of strain JC357 and to Muna A. Khan for construction of strain Z946. This work was supported by the 'Austrian Science Fund' (FWF) through the Special Research Program RNA-REG F43 under grant number F4317 (to B.G) and the Doktoratskolleg RNA Biology W1207-B09.

Disclosure statement

No potential conflict of interest was reported by the authors.

Funding

This work was supported by the Austrian Science Fund [Doktoratskolleg RNA Biology W1207-B09]; Austrian Science Fund [RNA-REG F43; F4317].

ORCID

Boris Görke  <http://orcid.org/0000-0002-1682-5387>

References

- [1] Arraiano CM, Andrade JM, Domingues S, et al. The critical role of RNA processing and degradation in the control of gene expression. *FEMS Microbiol Rev.* 2010;34:883–923.
- [2] Saramago M, Barria C, Dos Santos RF, et al. The role of RNases in the regulation of small RNAs. *Curr Opin Microbiol.* 2014;18C:105–115.
- [3] Evguenieva-Hackenberg E, Klug G. New aspects of RNA processing in prokaryotes. *Curr Opin Microbiol.* 2011;14:587–592.
- [4] Bandyra KJ, Luisi BF. RNase E and the high-fidelity orchestration of RNA metabolism. *Microbiol Spectr.* 2018;6:RWR-0008-2017.
- [5] Georg J, Dienst D, Schurgers N, et al. The small regulatory RNA SyR1/PsrR1 controls photosynthetic functions in cyanobacteria. *Plant Cell.* 2014;26:3661–3679.
- [6] Waters SA, McAteer SP, Kudla G, et al. Small RNA interactome of pathogenic *E. coli* revealed through crosslinking of RNase E. *Embo J.* 2017;36:374–387.
- [7] Lalaouna D, Eyraud A, Devinck A, et al. GcvB small RNA uses two distinct seed regions to regulate an extensive targetome. *Mol Microbiol.* 2019;111:473–486.
- [8] Kawamoto H, Morita T, Shimizu A, et al. Implication of membrane localization of target mRNA in the action of a small RNA: mechanism of post-transcriptional regulation of glucose transporter in *Escherichia coli*. *Genes Dev.* 2005;19:328–338.
- [9] Masse E, Escorcía FE, Gottesman S. Coupled degradation of a small regulatory RNA and its mRNA targets in *Escherichia coli*. *Genes Dev.* 2003;17:2374–2383.
- [10] Andreassen PR, Pettersen JS, Szczerba M, et al. sRNA-dependent control of curli biosynthesis in *Escherichia coli*: McaS directs endonucleolytic cleavage of *csgD* mRNA. *Nucleic Acids Res.* 2018;46:6746–6760.
- [11] Miyakoshi M, Chao Y, Vogel J. Regulatory small RNAs from the 3' regions of bacterial mRNAs. *Curr Opin Microbiol.* 2015;24:132–139.
- [12] Chao Y, Li L, Girodat D, et al. *In vivo* cleavage map illuminates the central role of RNase E in coding and non-coding RNA pathways. *Mol Cell.* 2017;65:39–51.
- [13] Dar D, Sorek R. Bacterial noncoding RNAs excised from within protein-coding transcripts. *MBio.* 2018;9.
- [14] Kim HM, Shin JH, Cho YB, et al. Inverse regulation of Fe- and Ni-containing SOD genes by a Fur family regulator Nur through small RNA processed from 3'UTR of the *sodF* mRNA. *Nucleic Acids Res.* 2014;42:2003–2014.
- [15] Eisenhardt KMH, Reuscher CM, Klug G. PcrX, an sRNA derived from the 3'-UTR of the *Rhodobacter sphaeroides puf* operon modulates expression of *puf* genes encoding proteins of the bacterial photosynthetic apparatus. *Mol Microbiol.* 2018;110:325–334.
- [16] De Mets F, Van Melderen L, Gottesman S. Regulation of acetate metabolism and coordination with the TCA cycle via a processed small RNA. *Proc Natl Acad Sci U S A.* 2019;116:1043–1052.
- [17] Miyakoshi M, Matera G, Maki K, et al. Functional expansion of a TCA cycle operon mRNA by a 3' end-derived small RNA. *Nucleic Acids Res.* 2019;47:2075–2088.
- [18] Papenfort K, Espinosa E, Casades J, et al. Small RNA-based feedforward loop with AND-gate logic regulates extrachromosomal DNA transfer in *Salmonella*. *Proc Natl Acad Sci U S A.* 2015;112:E4772–4781.
- [19] Guo MS, Updegrove TB, Gogol EB, et al. MicL, a new sigmaE-dependent sRNA, combats envelope stress by repressing synthesis of LPP, the major outer membrane lipoprotein. *Genes Dev.* 2014;28:1620–1634.
- [20] Papenfort K, Said N, Welsink T, et al. Specific and pleiotropic patterns of mRNA regulation by ArcZ, a conserved, Hfq-dependent small RNA. *Mol Microbiol.* 2009;74:139–158.
- [21] Mandin P, Gottesman S. Integrating anaerobic/aerobic sensing and the general stress response through the ArcZ small RNA. *Embo J.* 2010;29:3094–3107.
- [22] Fröhlich KS, Haneke K, Papenfort K, et al. The target spectrum of SdsR small RNA in *Salmonella*. *Nucleic Acids Res.* 2016;44:10406–10422.
- [23] Bandyra KJ, Said N, Pfeiffer V, et al. The seed region of a small RNA drives the controlled destruction of the target mRNA by the endoribonuclease RNase E. *Mol Cell.* 2012;47:943–953.
- [24] Del Campo C, Bartholomäus A, Fedyunin I, et al. Secondary structure across the bacterial transcriptome reveals versatile roles in mRNA regulation and function. *PLoS Genet.* 2015;11:e1005613.
- [25] Updegrove TB, Kouse AB, Bandyra KJ, et al. Stem-loops direct precise processing of 3' UTR-derived small RNA MicL. *Nucleic Acids Res.* 2018 [Epub ahead of print]. DOI:10.1093/nar/gky1175
- [26] Göpel Y, Khan MA, Görke B. Ménage à trois: post-transcriptional control of the key enzyme for cell envelope synthesis by a base-pairing small RNA, an RNase adaptor protein and a small RNA mimic. *RNA Biol.* 2014;11:433–442.
- [27] Urban JH, Vogel J. Two seemingly homologous noncoding RNAs act hierarchically to activate *glmS* mRNA translation. *PLoS Biol.* 2008;6:e64.
- [28] Kalamorz F, Reichenbach B, März W, et al. Feedback control of glucosamine-6-phosphate synthase GlmS expression depends on the small RNA GlmZ and involves the novel protein YhbJ in *Escherichia coli*. *Mol Microbiol.* 2007;65:1518–1533.
- [29] Gonzalez GM, Durica-Mitic S, Hardwick SW, et al. Structural insights into RapZ-mediated regulation of bacterial amino-sugar metabolism. *Nucleic Acids Res.* 2017;45:10845–10860.
- [30] Göpel Y, Papenfort K, Reichenbach B, et al. Targeted decay of a regulatory small RNA by an adaptor protein for RNase E and counteraction by an anti-adaptor RNA. *Genes Dev.* 2013;27:552–564.
- [31] Göpel Y, Khan MA, Görke B. Domain swapping between homologous bacterial small RNAs dissects processing and Hfq binding determinants and uncovers an aptamer for conditional RNase E cleavage. *Nucleic Acids Res.* 2016;44:824–837.
- [32] Reichenbach B, Maes A, Kalamorz F, et al. The small RNA GlmY acts upstream of the sRNA GlmZ in the activation of *glmS* expression and is subject to regulation by polyadenylation in *Escherichia coli*. *Nucleic Acids Res.* 2008;36:2570–2580.
- [33] Khan MA, Göpel Y, Milewski S, et al. Two small RNAs conserved in *Enterobacteriaceae* provide intrinsic resistance to antibiotics targeting the cell wall biosynthesis enzyme Glucosamine-6-phosphate synthase. *Front Microbiol.* 2016;7:908.
- [34] Reichenbach B, Göpel Y, Görke B. Dual control by perfectly overlapping sigma 54- and sigma 70- promoters adjusts small RNA GlmY expression to different environmental signals. *Mol Microbiol.* 2009;74:1054–1070.
- [35] Göpel Y, Görke B. Interaction of lipoprotein QseG with sensor kinase QseE in the periplasm controls the phosphorylation state of the two-component system QseE/QseF in *Escherichia coli*. *PLoS Genet.* 2018;14:e1007547.
- [36] Koralewska N, Hoffmann W, Pokornowska M, et al. How short RNAs impact the human ribonuclease Dicer activity: putative regulatory feedback-loops and other RNA-mediated mechanisms controlling microRNA processing. *Acta Biochim Pol.* 2016;63:773–783.
- [37] Wilson GG, Young KY, Edlin GJ, et al. High-frequency generalised transduction by bacteriophage T4. *Nature.* 1979;280:80–82.
- [38] Plumbridge JA, Cochet O, Souza JM, et al. Coordinated regulation of amino sugar-synthesizing and -degrading enzymes in *Escherichia coli* K-12. *J Bacteriol.* 1993;175:4951–4956.
- [39] Baba T, Ara T, Hasegawa M, et al. Construction of *Escherichia coli* K-12 in-frame, single-gene knockout mutants: the Keio collection. *Mol Syst Biol.* 2006;2:1–11.
- [40] Regnier P, Hajnsdorf E. Decay of mRNA encoding ribosomal protein S15 of *Escherichia coli* is initiated by an RNase E-dependent endonucleolytic cleavage that removes the 3' stabilizing stem and loop structure. *J Mol Biol.* 1991;217:283–292.
- [41] Bardey V, Vallet C, Robas N, et al. Characterization of the molecular mechanisms involved in the differential production of erythrose-4-phosphate dehydrogenase, 3-phosphoglycerate kinase and class II fructose-1,6-bisphosphate aldolase in *Escherichia coli*. *Mol Microbiol.* 2005;57:1265–1287.

- [42] Portier C, Migot C, Grumberg-Manago M. Cloning of *E. coli pnp* gene from an episome. *Mol Gen Genet.* 1981;183:298–305.
- [43] Goldblum K, Apririon D. Inactivation of the ribonucleic acid-processing enzyme ribonuclease E blocks cell division. *J Bacteriol.* 1981;146:128–132.
- [44] Schnetz K, Stülke J, Gertz S, et al. LicT, a *Bacillus subtilis* transcriptional antiterminator protein of the BglG family. *J Bacteriol.* 1996;178:1971–1979.
- [45] Temmel H, Müller C, Sauert M, et al. The RNA ligase RtcB reverses MazF-induced ribosome heterogeneity in *Escherichia coli*. *Nucleic Acids Res.* 2017;45:4708–4721.
- [46] Guzman LM, Belin D, Carson MJ, et al. Tight regulation, modulation, and high-level expression by vectors containing the arabinose P_{BAD} promoter. *J Bacteriol.* 1995;177:4121–4130.
- [47] Lüttmann D, Göpel Y, Görke B. The phosphotransferase protein EIIA^{Ntr} modulates the phosphate starvation response through interaction with histidine kinase PhoR in *Escherichia coli*. *Mol Microbiol.* 2012;86:96–110.
- [48] Lüttmann D, Heermann R, Zimmer B, et al. Stimulation of the potassium sensor KdpD kinase activity by interaction with the phosphotransferase protein IIA^{Ntr} in *Escherichia coli*. *Mol Microbiol.* 2009;72:978–994.
- [49] Guillier M, Gottesman S. Remodelling of the *Escherichia coli* outer membrane by two small regulatory RNAs. *Mol Microbiol.* 2006;59:231–247.
- [50] Callaghan AJ, Grossmann JG, Redko YU, et al. Quaternary structure and catalytic activity of the *Escherichia coli* ribonuclease E amino-terminal catalytic domain. *Biochemistry.* 2003;42:13848–13855.
- [51] Miller J. *Experiments in molecular genetics.* Cold Spring Harbor (NY): Cold Spring Harbor Laboratory Press; 1972.